Contribution of sodium dodecyl sulphate and sodium lauric acid in the one-pot synthesis of intercalated ZnAl-layered double hydroxides

FENGZHU LV*, ZILIN MENG, PENGGANG LI, YIHE ZHANG, GUOCHENG LV, QIAN ZHANG and **ZHILEI ZHANG**

State Key Laboratory of Geological Processes & Mineral Resources, National Laboratory of Mineral Materials, School of Materials Science and Technology, China University of Geosciences, Beijing 100083, China

Abstract. Anion surfactants, sodium dodecyl sulphate (SDS) and sodium lauric acid (SLA), with almost the same chain length but different anion groups were used together as intercalates to prepare intercalated ZnAl–layered double hydroxides (ZnAl–LDHs). Their composition, structure and morphology were characterized by Fourier transform infrared, X-ray fluorescence, thermogravimetric and X-ray diffraction (XRD). The results indicated SDS intended to maintain the lamellae structure of LDHs, but SLA was more likely to expand the basal spacings of LDHs in the present system. The arrangement of the surfactants in the interlayer of ZnAl–LDHs was also simulated by Materials Studio. The basal spacings of the LDHs calculated based on simulated structure consisted with that from XRD.

Keywords. ZnAl–LDHs; anionic surfactant; intercalation; molecular simulation.

1. Introduction

Layered double hydroxides (LDHs), also known as anionic or hydrotalcite-like clays, are a class of layered compounds that consist of positively charged brucite-like host layers and hydrated exchangeable anions located in the interlayer gallery for charge balance. The general structural formula for these compounds is $[M_{1-x}^{2+}M_x^{3+}(OH)_2]^{x+}$ $(A^{m-})_{x/m} \cdot n H_2O$, where M^{2+} and M^{3+} are divalent and trivalent cations. The value of x is equal to $M^{3+}/(M^{2+} + M^{3+})$ and A^{m-} is a charge balancing interlayer anion.[1] In most cases the x-values change between 0.10 and 0.33. These compounds exhibit an excellent ability to trap organic and inorganic anions due to the presence of positively charged brucite-like sheets, relatively weak interlayer bonding and ion-exchange properties.[2] These excellent properties are attractive for their wide applications, like catalysis,[3] drug and gene delivery,[4,5] pollutant scavenger,[2,6–8] etc.

Surfactant-intercalated LDHs, as one of the main types of LDHs, have been synthesized using several methods: (i) spontaneous self-assembly;[9] (ii) LDH reconstruction from a layered double oxide form obtained by calcinations of a suitable precursor;[10] and (iii) anion replacement by elimination of the precursor interlamellae species.[11] The spontaneous self-assembly method generally involves one-pot co-precipitation of LDH precursors in the presence of surfactants

using a base.[12–14] Compared with other approaches, the spontaneous self-assembly method shows great advantages because of its straight forward synthesis and mild reaction conditions. The fabrication process of surfactant-intercalated LDHs is a form of self-assembly that involves the trapping of guest molecules between layers in a crystal lattice during which the structural integrity of the latter is formally conserved. In principle, layered host lattices can adapt to the geometry of the inserted guest species by adjustment of the interlayer separation. For the spontaneous self-assembly method, LDHs layers and surfactants are closely interconnected. Therefore, organic anion intercalated LDHs with different chain lengths and different anions style are prepared by one pot synthesis, among which the intercalates are the salts of organic sulphate,[15] organic benzene sulphonic acid,[16] as well as monocarboxyl or dicarboxyl organic.[17] As organic carboxyl is intercalated, the prepared LDHs are mostly limited in MgAl–LDH. Although the arrangement of these organic anions in the interlayer of LDHs is clarified clearly. However LDHs with mixture of organic carboxyl and organic sulphate has not been reported.

In the present work, the mixture of sodium dodecyl sulphate (SDS) and sodium lauric acid (SLA), which almost have the same molecular length but different anionic groups, is used to prepare intercalated ZnAl–LDHs. The contributions of each surfactants on the fabrication of ZnAl–LDHs are studied. Also molecular simulation is used to study the arrangement of the surfactants in the interlayer. The basal spacing data from experiment and simulation are compared.

---

*Author for correspondence (lfz619@cugb.edu.cn)

2. Experimental

2.1 *Materials*

SDS and lauric acid were purchased from Xilong Chemical Corporation, China. Lauric acid was neutralized to sodium salt before use and the corresponding salt was assigned as SLA. $Zn(NO_3)_2 \cdot 6H_2O$ and $Al(NO_3)_3 \cdot 9H_2O$ were purchased from Jingwen Chemical Corporation, China. All other chemicals and reagents were purchased from Beijing Chemical Reagent Factory. They were analytical grade and used without further purification.

2.2 *Synthesis of surfactant-intercalated ZnAl–LDHs*

The intercalated ZnAl–LDHs with SDS, SLA, and the mixture of SDS and SLA as intercalates were synthesized according to the modified procedure.[18] The corresponding samples were assigned as ZnAl(SDS)–LDH, ZnAl(SLA)–LDH and ZnAl(*x/y*)–LDH, where *x/y* indicated the ratios of SDS to SLA which were 3/1, 1/1 and 1/3, respectively. The synthesis procedure for ZnAl(1/1)–LDH was as follows: 75 ml of SDS (1.73 g, 0.006 mol) and SLA (1.33 g, 0.006 mol) solution were mixed with 75 ml of $Zn(NO_3)_2 \cdot 6H_2O$ (5.95 g, 0.02 mol) and $Al(NO_3)_3 \cdot 9H_2O$ (3.75 g, 0.01 mol) solution. Under vigorous stirring, the pH of the obtained solution was adjusted to 10 by dropwise addition of a NaOH solution (1 mol l^{-1}). The derived suspension was maintained at 65°C for 8 h to complete the reaction. After aging for 12 h at room temperature, the resulting precipitate was collected by filtration, washed with pure water, and dried at 70°C.

2.3 *Characterization*

The wide- and small-angle X-ray diffraction (XRD) patterns were recorded on a Rigaku D/Max-rA rotating anode X-ray diffractometer equipped with a Cu-Kα tube and a Ni filter ($\lambda = 0.1542$ nm). Field-emission scanning electron microscopy (FE-SEM) analysis was conducted on a LEO-1530 FE-SEM operated at an acceleration voltage of 5 kV and connected with an EDX analyzer. The Fourier transform infrared (FT-IR) spectra in the region of 4000–400 cm^{-1} were obtained using a Perkin-Elmer Spectrum 100 FT-IR spectrometer. KBr was used as a background material. Thermal gravimetric analyses (TGA) were performed on a Perkin-Elmer TGA 7. The analysis scale was from room temperature to 800°C at a rate of 20°C min^{-1} in N_2. X-ray fluorescence (XRF) characterization was performed via a Rigaku ZSX Primus II spectroscopymeter. The Forcite module of Materials Studio 5.0 software was used to perform molecular simulation in order to investigate the SDS and SLA conformation in the interlayer of ZnAl–LDHs. The simulated temperature was 298 K, and time was 1 ns with a time step of 1 fs. After the system reached equilibrium, the NVT kinetic simulation was performed under the same time constant and temperature conditions.
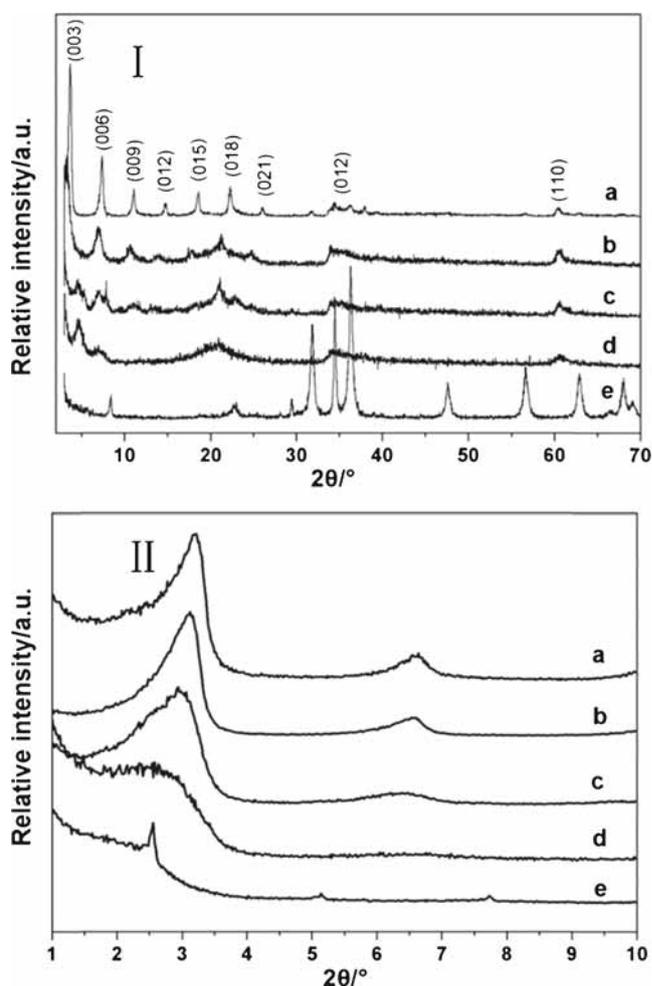

Figure 1. Wide-angle (I) and small-angle (II) XRD patterns of (**a**) ZnAl(SDS)–LDH, (**b**) ZnAl(3/1)–LDH, (**c**) ZnAl(1/1)–LDH, (**d**) ZnAl(1/3)–LDH and (**e**) ZnAl(SLA)–LDH.
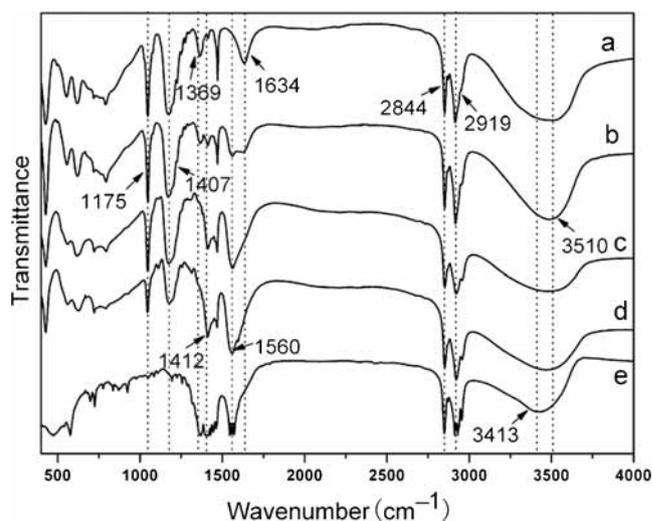

Figure 2. FT-IR spectra of (**a**) ZnAl(SDS)–LDH, (**b**) ZnAl(3/1)–LDH, (**c**) ZnAl(1/1)–LDH, (**d**) ZnAl(1/3)–LDH and (**e**) ZnAl(SLA)–LDH.

3. Results and discussion

The XRD patterns of all samples are shown in figure 1. Panels I and II are wide- and small-angle XRD patterns of the samples. Compared with typical reflections of ZnAl–LDHs reported in the literature,[18] the (003), (006) and (009) diffraction peaks of ZnAl(SDS)–LDH, ZnAl(3/1)–LDH, ZnAl(1/1)–LDH and ZnAl(1/3)–LDH in the wide XRD patterns shift to lower angle and match well with the organic–LDHs compound,[19] which indicates that larger SDS and SLA anions has intercalated to form surfactant-intercalated ZnAl–LDHs. But the wide XRD pattern of ZnAl(SLA)–LDH is different from the others. The peaks at 30–70° shown in figure 1e are consistent well with that of ZnO and the characteristic peaks of LDH fade away. While in the small-angle XRD pattern, (003), (006) and (009) diffraction of LDH still can be observed, indicating ZnAl(SLA)–LDH composes of ZnO and ZnAl–LDHs.

With the increase of SLA content, the (003) diffraction peaks of ZnAl–LDHs intercalated with the mixture of SLA and SDS in low-angle XRD patterns shift from 3.11° to 2.94°, then to 2.76° gradually, and the corresponding basal spacings are expanded to 2.83 nm (figure 1b), 2.98 nm (figure 1c) and 3.21 nm (figure 1d), respectively. The basal spacing of ZnAl(x/y)–LDHs increases with the content of SLA. SLA contributes more to expand the basal spacing of ZnAl(x/y)–LDHs.

Figure 2 shows the FT-IR spectra of ZnAl(SDS)–LDH, ZnAl(3/1)–LDH, ZnAl(1/1)–LDH, ZnAl(1/3)–LDH and ZnAl(SLA)–LDH. The vibration peaks at 2919 and 2844 cm^{-1} are due to the C–H stretching of SDS and SLA. The peaks at 1407 and 1175 cm^{-1} are the characteristics of SO_4^-. The peaks at 1412 and 1560 cm^{-1} contribute to the asymmetrical and symmetrical stretching vibrations of COO^-.[20] The appearance of these peaks suggests the incorporation of the surfactants into the LDHs.[21,22] The asymmetrical and
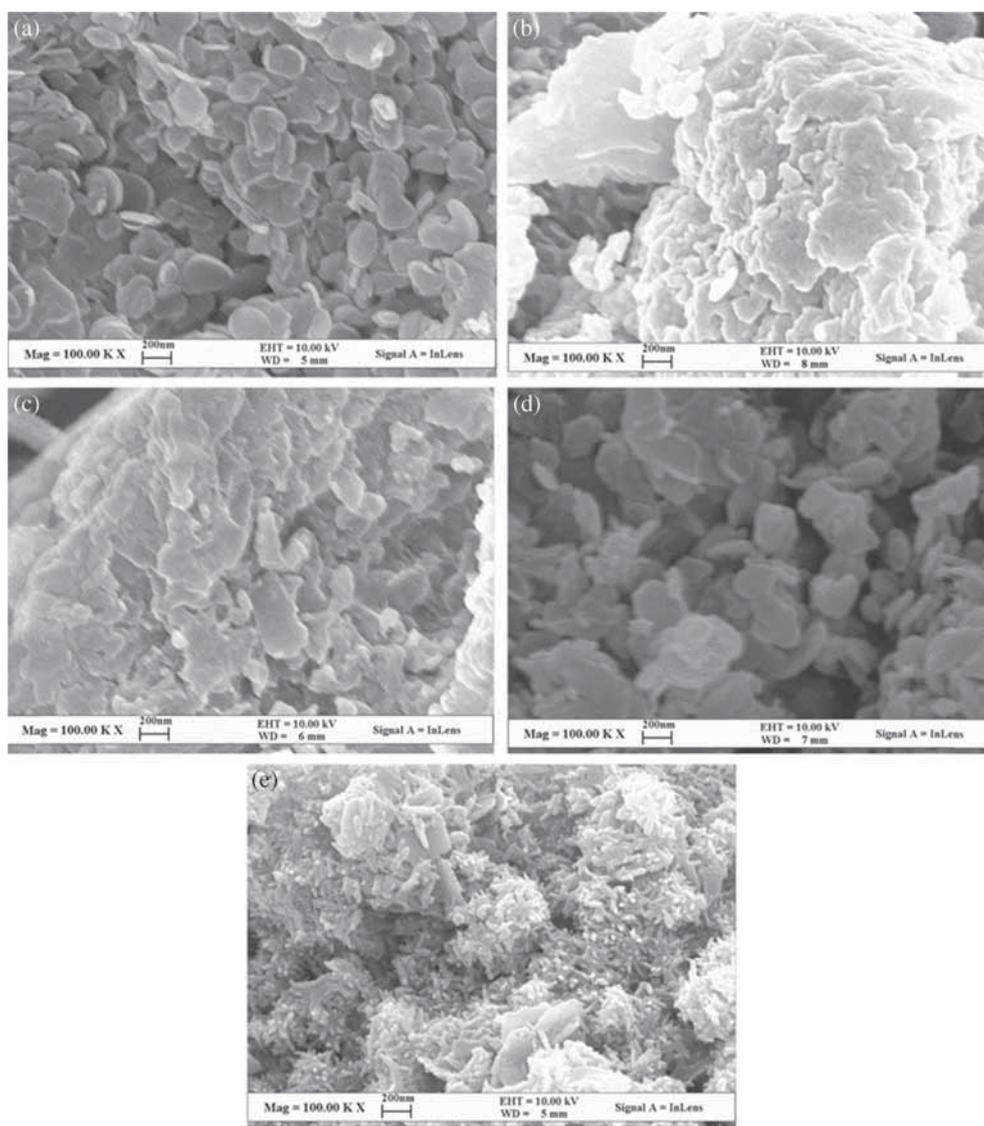

Figure 3. FE-SEM images of (**a**) ZnAl(SDS)–LDH, (**b**) ZnAl(3/1)–LDH, (**c**) ZnAl(1/1)–LDH, (**d**) ZnAl(1/3)–LDH and (**e**) ZnAl(SLA)–LDH.

symmetrical stretchings in the NO_3^- group results in strong absorption at 1634 and 1369 cm^{-1}, which are only shown in the curves of figure 2a and b. It manifests that in ZnAl(SDS)–LDH not all the LDH layer charges are balanced by SDS anions and some intercalates are NO_3^-. With the increase of SLA, the broad peak at 3510 cm^{-1} in the spectrum of ZnAl(SDS)–LDH from the vibration of –OH groups connected with metal ions shifts to 3413 cm^{-1} in the spectrum of ZnAl(SLA)–LDH. The disappearance of NO_3^- peaks and the large left shift of the –OH peaks indicate the interaction between SLA and LDH layers is greatly stronger than that between SDS and LDH layers. As the feeding proportion of SLA to SDS increases, the characteristic peaks of SDS (1407 and 1175 cm^{-1}) in the spectra of ZnAl(x/y)–LDH are weakened and that of SLA (1412 and 1559 cm^{-1}) become more obvious illustrating that more SLA get into the interlayer of LDHs and occupy the position of SDS.

The morphologies of the LDHs are shown in figure 3. As seen from figure 3a, the surface morphology of ZnAl(SDS)–LDH is lamellar plates stacking loosely to each other due to the weak particle–particle interactions. The products are almost hexagonal disks rather than regular hexagonal structure commonly observed for many LDHs.[23] The template effect of the surfactants is the primary cause to the non-hexagonal morphologies.[24] While in case of SLA, short rods, which is ZnO certified by XRD, occupy most of the view in figure 3e. In the preparation of ZnAl(SLA)–LDH, suspension of zinc laurates is generated in the process of adjusting pH of the reaction system due to the low solubility of zinc laurate (0.1 g l^{-1} at 15°C). But the morphologies of all ZnAl(x/y)–LDH (figure 3b–d) are still lamellae. Compared with ZnAl(SDS)–LDH, the layers of ZnAl(x/y)–LDH stack together densely and free layers can hardly be observed. The morphology of ZnAl(x/y)–LDH is lamellar and similar to ZnAl(SDS)–LDH but obviously different from that of ZnAl(SLA)–LDH, indicating the lamellar template effect of SDS is higher than SLA. As the strong interaction between Zn^{2+} and SLA or the precipitation effect of Zn^{2+} with SLA can be greatly limited as SLA together with SDS as intercalates. So in the fabrication processes of ZnAl(x/y)–LDHs, SDS show great contribution to the lamellar structure formation.

The measured chemical compositions, calculated atomic ratio and proposed formulae of ZnAl(SDS)–LDH, ZnAl(3/1)–LDH, ZnAl(1/1)–LDH and ZnAl(1/3)–LDH based on the XRF measurement are shown in table 1. The feeding ratio of Zn to Al is two, while the ratios of Zn to Al in the final samples are all higher than the feeding ratio or the theoretical one, and close to 3, except ZnAl(SLA)–LDH. The higher ratio of Zn to Al is caused by the strong amphoteric property of Al as well as the non-accurate controlling of pH. As the final suspension is alkali (pH = 10), some Al elements are changed to $[Al(OH)_4]^-$ and dissolved in solution. The even more higher ratio of Zn to Al in ZnAl(SLA)–LDH is due to the strong interaction of Zn^{2+} with SLA due to which rod ZnO forms (XRD and SEM results). The ratios of SDS to SLA in ZnAl(x/y)–LDHs are almost equal to the theory value. The reason why the other samples are not influenced by the low solubility of zinc laurate is that SDS and SLA in solution self-assembling into micelles, the interaction of SLA with Zn cannot separate SLA from the micelles due to the strong hydrophobic interaction of micelle core, which is a strong evidence of the vital function of micelles in the self-assembly method for preparation of surfactant-intercalated LDHs in the one pot process. The positive charges of ZnAl–LDH sheets come from the replacement of Zn^{2+} by Al^{3+} in the LDH lattice in which the charge formed by each of the substitution requires one anion surfactant to balance. Therefore, the proposed formulae are based on the chemical compositions and the relationship of Al^{3+} with surfactants. The proposed formulae are used to structural optimization in the molecular simulation process. It should be point out that
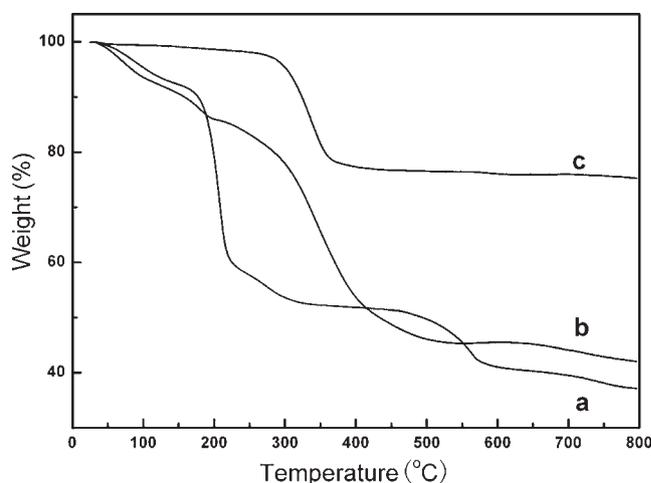

Figure 4. TGA curves of (**a**) ZnAl(SDS)–LDH, (**b**) ZnAl(1/1)–LDH and (**c**) ZnAl(SLA)–LDH.

Table 1. Compositions of the synthesized ZnAl–LDHs.

| LDH	Chemical compositions (mol)			Atomic ratio		Proposed formulae
	Zn	Al	S	Zn/Al	SDS/SLA	
ZnAl(SDS)–LDH	0.729	0.241	0.205	3.02		$[Zn_{0.75}Al_{0.25}(OH)_2](C_{12}H_{25}SO_4^-)_{0.205}(NO_3)_{0.045}$
ZnAl(3/1)–LDH	0.743	0.262	0.195	2.84	2.91	$[Zn_{0.74}Al_{0.26}(OH)_2](C_{12}H_{25}SO_4^-)_{0.195}(C_{11}H_{21}COO^-)_{0.065}$
ZnAl(1/1)–LDH	0.921	0.251	0.137	3.66	1.20	$[Zn_{0.78}Al_{0.22}(OH)_2](C_{12}H_{25}SO_4^-)_{0.137}(C_{11}H_{21}COO^-)_{0.114}$
ZnAl(1/3)–LDH	0.863	0.253	0.07	3.41	0.38	$[Zn_{0.77}Al_{0.23}(OH)_2](C_{12}H_{25}SO_4^-)_{0.070}(C_{11}H_{21}COO^-)_{0.183}$
ZnAl(SLA)–LDH	1.082	0.022		49.2		—
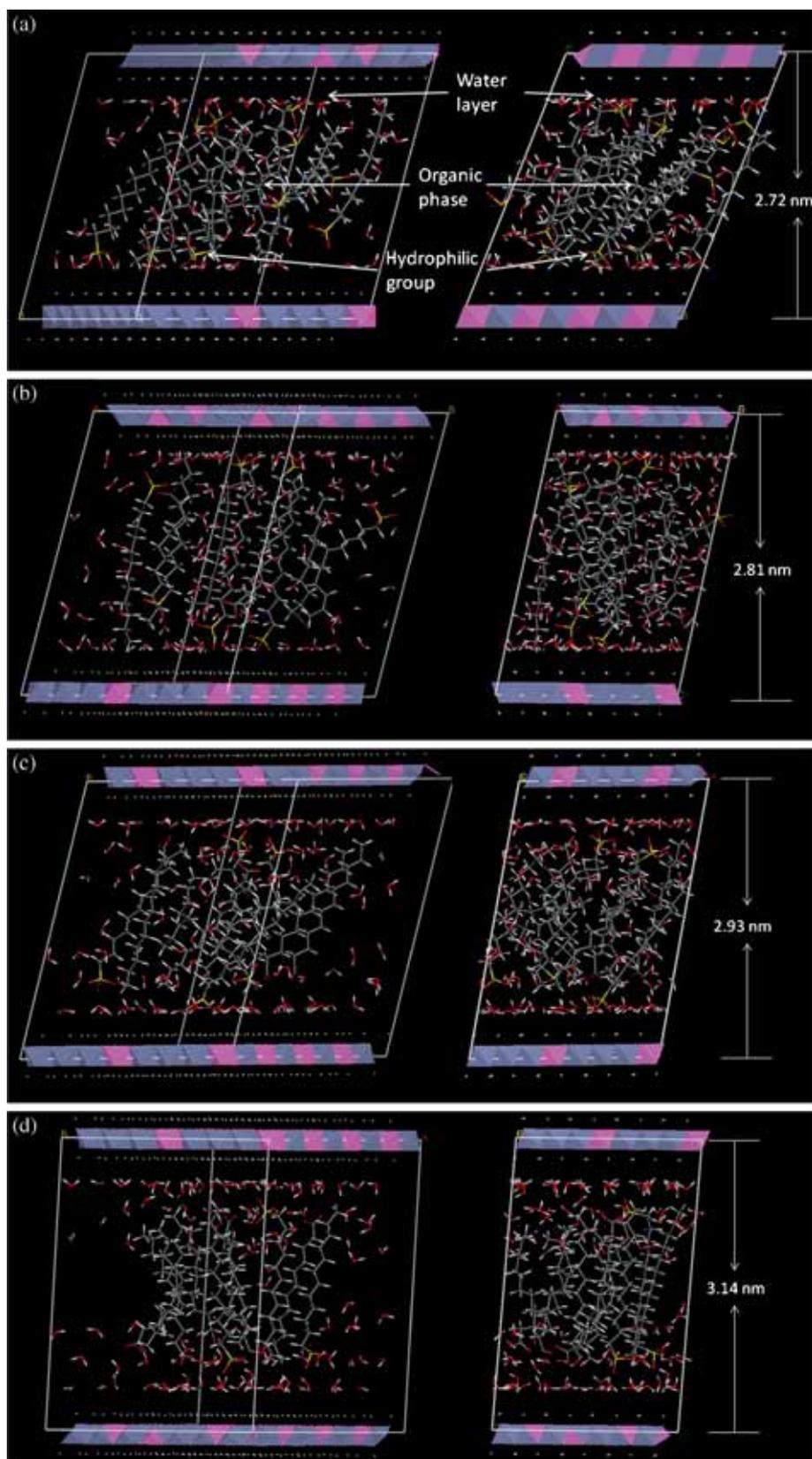
Figure 5. Simulated structure of (**a**) ZnAl(SDS)–LDH, (**b**) ZnAl(3/1)–LDH, (**c**) ZnAl(1/1)–LDH and (**d**) ZnAl(1/3)–LDH.

the formulae of ZnAl(3/1)–LDH proposed is not very accurate since FT-IR results indicate there are NO_3^- in ZnAl(3/1)–LDH, which could not be tested out accurately by XRF and not considered in the present work. No XRF signal of ZnAl(3/1)–LDH suggests only little amount of NO_3^- in ZnAl(3/1)–LDH therefore can be ignored.

For understanding the amount of the surfactants in the system and testing the accuracy of the proposed formulae, TGA measurement is carried out. ZnAl(SDS)–LDH shows a three-step degradation mechanism (figure 4a). The first step (25–150°C) corresponds to the removal of physical absorbed and interlayer water molecules. The major and important step takes place at 170–300°C due to the degradation of SDS and dehydroxylation of the LDH sheets. The last step is in the range of 450–600°C corresponding to the NO_3^- and sulphate deriving from the degradation of SDS.[21] For ZnAl(1/1)–LDH (figure 4b), the weight loss also can be divided into three steps. The first step before 170°C also corresponds to the removal of physical absorbed and interlayer water. The gradual weight loss at 300–450°C is due to the removal of SDS, SLA and dehydroxyed water. Up to 700°C, the residue of ZnAl(SDS)–LDH is 41% and almost equal to that of ZnAl(1/1)–LDH. For ZnAl(SDS)–LDH the weight loss corresponding to SDS degradation at 170–300°C is about 35 wt% which is consistent well with the content of SDS in ZnAl(SDS)–LDH (37.0 wt%) based on the formula of $[Zn_{0.75}Al_{0.25}(OH)_2](C_{12}H_{25}SO_4^-)_{0.205}(NO_3)_{0.045}$. So the formula of ZnAl(SDS)–LDH is accurate and the formulae of ZnAl(1/3)–LDH, ZnAl(1/1)–LDH and ZnAl(3/1)–LDH afforded are preferred to be accurate. While the weight loss cure of ZnAl(SLA)–LDH only shows one step at 300–400°C contributing to the degradation of SLA.[25]

The supercell of the model is established based on the data of XRF and the afforded formulae as shown in table 1 and optimized geometrically. After the system reached equilibrium, the kinetic simulation was performed and the results are shown in figure 5. It is should be pointed out that as ZnAl(SLA)–LDH is mixed a lot of ZnO showed in the result of XRD and SEM, so there is no accurate data for molecular simulation of ZnAl(SLA)–LDH. It can be seen that the surfactant monolayer in the interlayer of all the samples is formed in an anti-parallel arrangement[26] no matter SDS or SLA is used alone or together. The simulated structure of ZnAl–LDHs shows there is water layer existing between the surfactant layer and the LDH sheets. So the surfactants form hydrated monolayers[27] and the morphology of the surfactants in the interlayer can be considered as a normal micelle (figure 5).

The results of molecular simulation also show that the basal spacing of ZnAl(SDS)–LDH, ZnAl(3/1)–LDH, ZnAl(1/1)–LDH and ZnAl(1/3)–LDH increase from 2.72 nm to 2.81, 2.93 and 3.14 nm and the corresponding tilt angle of the surfactant chain to LDH sheets increase from 69.13° to 79.49°, 84.22° and 85.54°. These data confirm that the basal spacing increase of ZnAl(x/y)–LDHs is due to the tilt angle change rather than the arrangement of surfactant from anti-parallel form to dilayer form. The vertical arrangement

confirms that the interaction of LDH sheets with SLA and SDS, which is compensated by the hydrophobic interaction of SLA and SDS layers, is stronger than that of SDS with LDH. The sulphur atom in $R\text{-}SO_4^-$ is sp^3 hybridization and two S–O from $R\text{-}SO_4^-$ can form p–d π bonds. Due to the π bond, the attracting electron capability of sulphur atom from hydroxyl is enhanced and the positive charge in the sulphur atom is diminished. So $R\text{-}SO_4^-$ is more stable than $R\text{-}COO^-$ and $R\text{-}COO^-$ is more like attraction cations. Hence the interaction of SLA with LDH is stronger than in the case of SDS. SLA is more like escaping from the core of LDH therefore plays a leading role to expanding of the basal spacing of ZnAl–LDHs.

4. Conclusions

Intercalated ZnAl–LDHs using SDS and SLA mixtures as intercalates are prepared via one pot synthesis. The composition, structure and morphology characterization of the intercalated ZnAl–LDHs indicated SDS intended to maintain the lamellae structure of LDHs, but SLA is more like to expanding the basal spacing of LDHs in the present system although the two molecules possessed almost the same molecule length. The arrangement of the surfactants in the interlayer of ZnAl–LDHs is also simulated by Materials Studio. And the calculated basal spacing of the LDHs based on simulated structure was consistent well with that from XRD. The basal spacing of the intercalated ZnAl–LDHs can be adjusted by variation the ratio of SDS to SLA.

References

1. Arco M, Gutiérrez S, Martín C, Rives V and Rocha J 2004 *J. Solid State Chem.* **177** 3954
2. Goh K H, Lim T T and Dong Z 2008 *Water Res.* **42** 1343
3. Xia S J, Liu F X, Ni Z M, Xue J L and Qian P P 2013 *J. Colloid. Interf. Sci.* **405** 195
4. Li A, Qin L, Wang W, Zhu R, Yu Y, Liu H and Wang S 2011 *Biomaterials* **32** 469
5. Panda H S, Srivastava R and Bahadur D 2009 *J. Phys. Chem. B* **113** 15090
6. Cornejo J, Celis R, Pavlovic I and Ulibarri M A 2008 *Clay Miner.* **43** 155
7. Pavan P C, Crepaldi E L and Valim J B 2000 *J. Colloid. Interface Sci.* **229** 346
8. Lv F Z, Wu Y Y, Zhang Y H, Shang J W and Chu P K 2012 *J. Mater. Sci.* **47** 2033
9. Chen W, Li F and Qu B J 2004 *Chem. Mater.* **16** 368

10. Valente J S, Lima E, Toledo-Antonio J A, Cortes-Jacome M A, Lartundo-Rojas L, Montiel R and Prince J 2010 *J. Phys. Chem. C* **114** 2089

11. Liang J B, Ma R, Geng F X, Ebina Y and Sasaki T 2010 *Chem. Mater.* **22** 6001

12. Chen W and Qu B 2004 *J. Mater. Chem.* **14** 1705

13. Hsueh H B and Chen C Y 2003 *Polymer* **44** 1151

14. Tao Q, He H P, Frost R L, Yuan P and Zhu J X 2009 *Appl. Surf. Sci.* **255** 4334

15. Pavan P C, Gomes G D A and Valim J B 1998 *Microporous Mesoporous Mater.* **21** 659

16. Li P G, Lv F Z, Xu Z X, Qi G G and Zhang Y H 2013 *J. Mater. Sci.* **48** 5437

17. Saber O and Tagaya H 2003 *J. Incl. Phenom. Macrocyclic Chem.* **45** 107

18. Grover K, Komarneni S and Katsuki H 2010 *Appl. Clay Sci.* **48** 631

19. Fudala A, Palinko I and Kiricsi I 1999 *Inorg. Chem.* **38** 4653

20. Zhang J, Zhang F Z, Ren L L, Evans D G and Duan X 2004 *Mater. Chem. Phys.* **85** 207

21. You Y W, Zhao H T and Vance G F 2002 *Colloids Surf. A* **205** 161

22. Guo Y, Zhang H, Zhao L, Li G D, Chen J S and Xu L 2005 *J. Solid State Chem.* **178** 1830

23. Liu Z P, Ma R Z, Osada M, Nobuolyi Ebina Y, Takada K and Sasaki T S 2006 *J. Am. Chem. Soc.* **128** 4872

24. Yilmaz C, Unal U and Acar H Y 2012 *J. Solid State Chem.* **187** 295

25. Anbarasan R, Lee W and Soon S I 2008 *J. Serb. Chem. Soc.* **73** 321

26. Wang D Y, Costa F R, Vyalikh A, Leuteritz A, Scheler U, Jehnichen D, Wagenknecht U, Häussler L and Heinrich G 2009 *Chem. Mater.* **21** 4490

27. Carlino S 1997 *Solid State Ion.* **98** 73